Int. J. Heat Mass Transfer. Vol. 7, pp. 1405–1417. Pergamon Press 1964. Printed in Great Britain

DECELERATION AND MASS CHANGE OF AN ABLATING BODY DURING HIGH-VELOCITY MOTION IN THE ATMOSPHERE*

CARL GAZLEY Jr.
The RAND Corporation, Santa Monica, California

(*Received* 3 *August* 1964)

Abstract—This paper examines the factors affecting the dynamics and mass loss of ablating bodies during high-velocity motion. The dynamics and ablation of the body are interdependent since the rate of mass loss depends on the velocity and since the deceleration is dependent on the ratio of mass to drag area (m/C_DA) which may change due to loss of mass and change of shape. The initial kinetic energy of the body decreases due to both a loss of mass and a loss of velocity. The relative rates of mass loss and velocity loss depend on the "efficiency" with which the energy lost due to fluidynamic drag is returned to the body and absorbed in the ablation process.

The classic meteor case, where the flow is assumed to be of the free-molecule type with constant heat-transfer and drag coefficients, is reviewed and presented in terms of general dimensionless parameters which allow application to cases other than that of meteor atmospheric entry. This solution indicates a finite mass remaining after the deceleration, the magnitude of the mass relative to the initial mass depending on the "efficiency" described above.

In general, cases with variable heat-transfer and drag coefficients require numerical machine solutions (now in progress). However, analytic solutions for certain cases are possible and are presented in this paper. An analytic solution is obtained for the specific variation of the heat-transfer coefficient corresponding to a sphere with laminar convective heating in hypersonic flight at a constant altitude. In this case, the increase of dimensionless heat-transfer coefficient due to decreasing body size (thus effectively increasing the "efficiency") can result in a complete loss of mass during the deceleration process.

For both this case and the meteor case, the velocity variation during the major part of the mass loss differs only slightly from that for a body with an unchanging ballistic coefficient (m/C_DA). This approximation is used to formulate the analytic solution of a case which corresponds to the laminar convective heating of a sphere in hypersonic re-entry—i.e. a large slow meteor or fireball. Due to the dominant effect of the decrease in heat-transfer coefficient with increasing fluid density (thus effectively decreasing the "efficiency"), the rate of mass loss is reduced and the final mass is appreciable compared to the initial mass. The analytic results are compared with two well-observed fireballs.

NOMENCLATURE

A, cross-sectional frontal area of body;
C_D, aerodynamic drag coefficient;
C_{D_i}, initial value of drag coefficient;
$\overline{C_D}$, drag-coefficient ratio $= C_D/C_{D_i}$;
C_H, dimensionless heat-transfer coefficient;
C_{H_i}, initial value of heat-transfer coefficient;
$\overline{C_H}$, ratio $= C_H H_i/(C_{H_i} H)$;
D, characteristic dimension of body, changing dimension of body;
D_i, initial body dimension;
$\bar{D}$, dimensionless body size;
e, base of natural logarithms;
h, altitude;
H, effective heat of ablation;
H_i, initial value of H;
I, luminous intensity;
m, mass of body;
m_i, initial mass of body;
$\bar{m}$, dimensionless mass ratio $= m/m_i$;
n, geometry parameter, see equation (6);
q, heat-transfer rate to body;
u, velocity of body;
u_i, initial velocity of body;

* This paper was presented at the Second All-Union Conference on Heat and Mass Transfer in Minsk, 4–9 May 1964.

$\bar{u}$, dimensionless velocity ratio $= u/u_i$;
x, distance along path.

Greek symbols

α, reciprocal of density scale height ($\alpha = \mathrm{d}\ln\rho/\mathrm{d}h$);
Λ, dimensionless mass of air encountered per unit cross-sectional area $= \lambda/(m/C_DA)_i$;
ϕ, dimensionless factor $= C_{H_i}u_i^2/(2C_{D_i}H_i)$;
ρ, atmospheric density;
ρ_{SL}, atmospheric density at sea level;
σ, density ratio, ρ/ρ_{SL};
θ, flight path angle with respect to local horizontal (positive for descent, negative for ascent);
τ, luminous efficiency.

I. INTRODUCTION

FOR MANY years ballisticians have been concerned with the motion of bodies in the Earth's atmosphere—bodies of constant shape, size, and mass. With the advent of higher flight speeds with large rates of aerodynamic heating, the body may suffer a loss in mass due to surface ablation and a consequent change in shape and size. This effects a change in the ballistic coefficient with a consequent change in the body's dynamics and a corresponding change in the subsequent aerodynamic heating and mass loss. This coupling between the dynamics and ablation introduces a number of complications into the solution of the equations for the dynamics and mass loss. While machine solutions are generally necessary, analytic solutions have been possible in a few cases. Notable among these is the case of a body in a free-molecule flow (the typical meteor case) which is simplified by the lack of dependence of the aerodynamic drag and heat-transfer coefficients on the size and shape of the body. The solution to the meteor problem was first obtained by Hoppe [1] and Levin [2]. As Bronshten [3] has recently pointed out, larger meteoric bodies penetrate deeper into the atmosphere and consequently into the continuum flow regime.

In this paper, the drag and heating relations are developed in a general form and analytic solutions for certain cases are presented.

II. ANALYSIS

Aerodynamic heating and ablation

The heating rate to the body can be expressed as

$$q = C_H A \tfrac{1}{2}\rho u^3 \tag{1}$$

where C_H is a dimensionless heat-transfer coefficient and is the fraction of the kinetic energy of the air (relative to the body) intercepted by the body which reaches the body surface as heat. The rate of mass loss due to ablation may be approximated by the use of the "effective heat of ablation", H, which absorbs the effects of the various factors affecting the interaction between the flow about the body and the body surface. This is defined as

$$-\frac{\mathrm{d}m}{\mathrm{d}t} = \frac{q}{H} \tag{2}$$

where q in each of these equations is the heating rate which a non-ablating body would experience under the same flight conditions. The effects of the ablation in sometimes reducing the heat input is absorbed in H. The rate of mass loss is then

$$-\frac{\mathrm{d}m}{H} = \frac{C_H A}{\mathrm{d}t}\tfrac{1}{2}\rho u^3. \tag{3}$$

It is now useful to introduce a new independent variable, the mass of air encountered per unit frontal area during the flight (made dimensionless through division by the initial ballistic coefficient)

$$\Lambda = \frac{\int \rho\, u\, \mathrm{d}t}{(m/C_DA)_i}.$$

It is also convenient to introduce the dimensionless parameters

$$\bar{m} = \frac{m}{m_i}$$

$$\bar{u} = \frac{u}{u_i}$$

$$\overline{C_D} = \frac{C_D}{C_{D_i}}$$

$$\overline{C_H} = \frac{C_H H_i}{C_{H_i} H}$$

$$\bar{A} = \frac{A}{A_i}$$

$$\phi = \frac{C_{H_i} u_i^2}{2 \overline{C_{D_i}} H_i}$$

Then equation (3) becomes

$$-\frac{\mathrm{d}\bar{m}}{\mathrm{d}\Lambda} = \phi \, \overline{C_H} \, \bar{A} \, \bar{u}^2 \qquad (4)$$

The dimensionless drag and heat-transfer coefficients may vary appreciably during a body's flight—the variation being due to both changes in the flow regime and in the shape of the body. Furthermore, the effective heat of ablation, H, will change with both the flow regime and the heating rate. Figure 1 shows schematically how these parameters may vary with altitude [8].

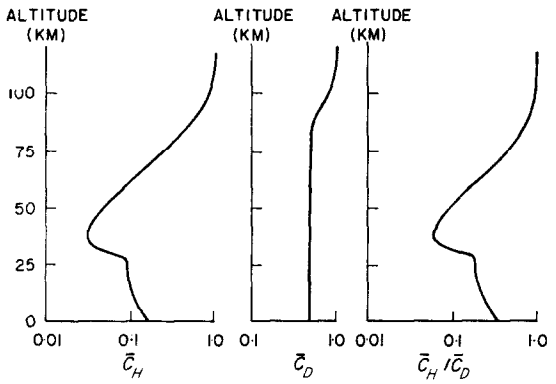

FIG. 1. Schematic variation of the dimensionless heat-transfer and drag coefficient ratios.

Body geometry

We shall consider a body of uniform density and arbitrary geometry having a characteristic dimension, D, which varies due to ablation. For example, a randomly spinning sphere undergoing ablation will suffer a decrease in diameter. Its mass is

$$m = \frac{\pi}{6} \rho_s D^3$$

and its frontal area is

$$A = \frac{\pi}{4} D^2.$$

The resulting mass–area ratio is

$$\frac{m}{A} = \frac{2}{3} \rho_s D$$

and the relation between mass and mass–area ratio is

$$m = \frac{9\pi}{16 \rho_s^2} \left(\frac{m}{A}\right)^3.$$

In general, for other geometric shapes, the mass is proportional to a power of the changing dimension

$$\bar{m} = \bar{D}^n \qquad (5)$$

and the mass–area ratio is directly proportional to the changing dimension

$$\frac{\bar{m}}{\bar{A}} = \bar{D}.$$

Thus the mass and area are related

$$\bar{m} = \bar{A}^{n/(n-1)}$$

and

$$\bar{m} = \left(\frac{\bar{m}}{\bar{A}}\right)^n. \qquad (6)$$

These relations evolve from the fact that ablation occurs on the forward-facing surfaces and is approximately proportional to frontal area [see equations (3) and (4)]. Values of the exponent n are given in Table 1 for various simple geometries.

Table 1

n	Geometry
1	Rectangular solid moving normal to one face, or cylinder moving axially
2	Cylinder moving normal to axis
3	Spinning sphere, or cone moving axially

Deceleration

The deceleration experienced by the body may be expressed in terms of the aerodynamic drag coefficient

$$-\frac{\mathrm{d}u}{\mathrm{d}t} = \frac{C_D A}{m} \tfrac{1}{2} \rho u^2 \qquad (7)$$

This equation neglects any gravitational acceleration which, for the velocity regime being considered, is negligible compared to that due to aerodynamic drag. Writing this equation with (u^2) as the dependent variable

$$\frac{d(u^2)}{dt} = \frac{C_D A}{m} \rho u^3$$

and introducing the dimensionless variables gives

$$-\frac{d\bar{u}^2}{d\Lambda} = \frac{\bar{C}_D \bar{A}}{\bar{m}} \bar{u}^2. \tag{8}$$

For a constant ballistic coefficient, $\bar{C}_D \bar{A}/\bar{m} = 1$, this equation can be integrated directly to give

$$\ln \bar{u}^2 = -\Lambda$$

or

$$\bar{u} = \exp[-\Lambda/2] \tag{9}$$

This will not be recognized as the familiar solution for ballistic re-entry into an isothermal atmosphere [4, 5] when it is noted that

$$\Lambda = \rho C_D A/(\alpha m \sin\theta).$$

In the case of motion at a constant altitude, $\Lambda = \rho x/(m/C_D A)$, i.e. Λ is directly proportional to x, the distance traveled. It is perhaps useful at this point to develop the significance of the parameter $\Lambda = \int \rho u \, dt/(m/C_D A)_i$, which is the ratio of the mass of gas encountered by the body per unit frontal area in ratio to the body's (initial) mass per unit drag area. As indicated by equation (9), the velocity has been reduced to about 61 per cent of its original value when $\Lambda = 1$. At $\Lambda = 2$, the velocity has been reduced to $1/e$ of its original value. This parameter can be considered qualitatively as a dimensionless mean free path. A non-ablating body can effectively penetrate a gas mass equivalent to a value of Λ somewhat greater than unity (say four or five). However, in the present case, we are concerned with a body whose size and mass are varying due to ablation and the integration of equation (8) can only be accomplished if these variations are taken into account. Combining the variations in mass and area by means of equation (6) gives

$$\bar{m} = \left(\frac{\bar{m}}{\bar{A}}\right)^n$$

and equation (8) can be expressed as

$$-\frac{d\bar{u}^2}{d\Lambda} = \bar{C}_D \bar{u}^2 (\bar{m})^{-1/n}. \tag{10}$$

In general, numerical integration [with simultaneous solution of equations (4) and (8)] is necessary; however, an analytic solution is possible for the case where $C_H/(C_D H)$ is constant. This is described in the next section.

Analytic solution for constant $\overline{C_H}/\overline{C_D}$

While considerable variation in the heat-transfer and drag coefficients and in their ratio can occur if the body moves through widely different regimes of gas density and body velocity or if the body suffers large changes in size and shape, there are a number of occasions where a solution for constant $\overline{C_H}/\overline{C_D}$ is useful. The meteor case is an example—small bodies decelerating in the upper atmosphere in the free-molecule flow regime. An analytic solution for this case was first obtained by Hoppe [1] and Levin [2] and will be presented here in terms of the general parameters, ϕ and Λ.

Eliminating the variable Λ between equations (4) and (8) gives

$$\frac{d \ln \bar{m}}{d\bar{u}^2} = \phi \frac{\overline{C_H}}{\overline{C_D}}. \tag{11}$$

Providing the combination of parameters on the right-hand side of this equation is constant (i.e. $\overline{C_H}/\overline{C_D} = 1$), direct integration is possible and gives

$$\ln \bar{m} = -\phi(1 - \bar{u}^2)$$

or

$$\bar{m} = \exp[-\phi(1 - \bar{u}^2)]. \tag{12}$$

It is interesting to note that, for this case, the mass variation is dependent only on the velocity, the initial velocity, and the parameter ϕ. Equation (12) is shown graphically in Fig. 2 (for convenience ϕ/n is used and the curves shown correspond to $n = 3$) and it will be noted that a finite mass remains at the end of the deceleration

$$\bar{m}_f = \exp -\phi.$$

Inserting equation (12) into equation (10) gives

$$-\frac{d\bar{u}^2}{d\Lambda} = \overline{C_D} \bar{u}^2 \exp[\phi/n(1 - \bar{u}^2)]$$

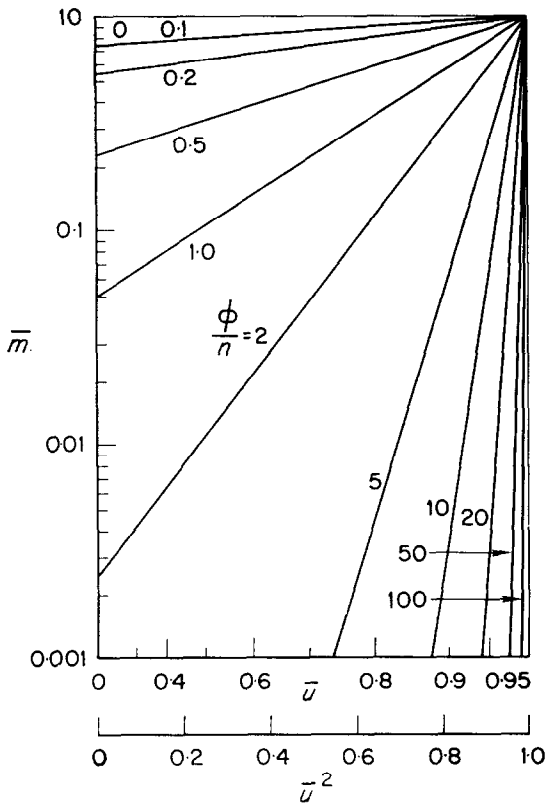

FIG. 2. Variation of mass with velocity for constant $\overline{C_H}/\overline{C_D}$ ($n = 3$).

or in integral form

$$-\int_1^{\bar{u}} \frac{\exp\left[(\phi/n)\,\bar{u}^2\right]\mathrm{d}\bar{u}^2}{\bar{u}^2} = \exp\left[\phi/n\right]\int_0^{\Lambda} \overline{C_D}\,\mathrm{d}\Lambda.$$

With the additional assumption of constant drag coefficient ($\overline{C_D} = 1$), this can be integrated to yield

$$\Lambda \exp\left(\phi/n\right) = \overline{Ei}\left(\frac{\phi}{n}\right) - \overline{Ei}\left(\frac{\phi}{n}\bar{u}^2\right) \qquad (13)$$

where $\overline{Ei}(\ )$ is the exponential integral

$$\overline{Ei}(x) = \int_{-\infty}^{x} \frac{\exp(x)\,\mathrm{d}x}{x}.$$

While equations (12) and (13) are applicable only to those cases where $\overline{C_H}/\overline{C_D} = 1{\cdot}0$ (e.g. the meteor case where $\overline{C_H} = \overline{C_D} = 1{\cdot}0$ because of free-molecule flow or the case of a body such as a hemisphere-cylinder moving at a constant altitude), the results are qualitatively similar to those for more complex cases. Because of this, they will be examined in some detail so as to give a physical feeling for the processes occurring and so as to provide a standard of comparison.

The variations of velocity and of mass with the parameter Λ are shown in Fig. 3 for several values of ϕ/n. It is seen that as ϕ/n increases, the deceleration and mass loss are shifted to smaller values of Λ. For $\phi/n = 0$, there is no mass loss and the velocity variation reduces to equation (9). The variation of the mass-velocity ratio is shown in Fig. 4 and it is seen that for small values of ϕ the velocity loss predominates while the larger values of ϕ result in a relatively large mass loss before the deceleration becomes appreciable. It will be remembered that $\phi = C_{H_i}u_i^2/(2C_{D_i}H_i)$ is essentially the product of two ratios: C_{H_i}/C_{D_i}

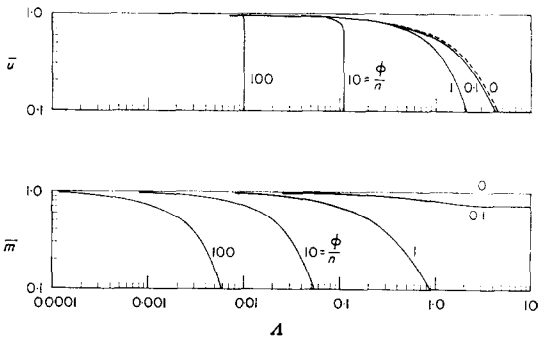

FIG. 3. Variation of velocity and mass with Λ for constant $\overline{C_H}/\overline{C_D}$ ($n = 3$).

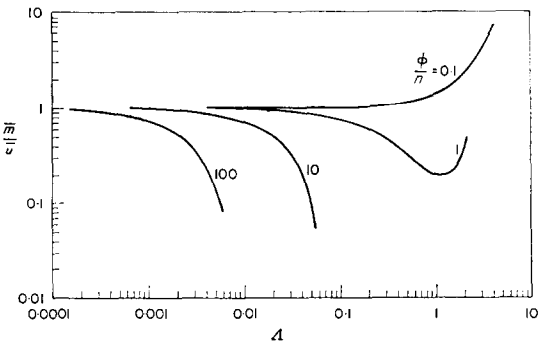

FIG. 4. Variation of mass–velocity ratio with Λ for constant $\overline{C_H}/\overline{C_D}$ ($n = 3$).

is the fraction of the drag energy which reaches the body as heat, and $(u_i^2/2)/H_t$ is the ratio of the specific kinetic energy initially possessed by the body to the energy necessary to ablate it. The product is thus essentially a ratio of the energy available for ablation to that required for ablation and can be considered as an efficiency of ablation. For high ablation efficiencies, mass loss tends to be the dominant process; for low efficiencies, deceleration is dominant.

Perhaps the best physical feeling for the relative importance of these competing processes is realized from Fig. 5 which presents lines of constant mass ratio and velocity ratio in the ϕ–Λ plane. In this plane, the process proceeds along a horizontal line—i.e. a constant value of ϕ. For very small values of ϕ there is seen to be only a small mass loss with a velocity variation essentially the same as the solution for constant $m/C_D A$, indicated by the broken vertical lines at the bottom of Fig. 5. At larger values of ϕ, the mass loss becomes more severe with a consequent greater deceleration. For still larger values of ϕ, essentially all of the mass loss takes place before any appreciable deceleration occurs; thereafter, deceleration is severe and takes place in a very small distance—i.e. in a small range of Λ.

At large values of ϕ where severe mass loss occurs before any appreciable deceleration, considerable simplification in the solution results. Thus for $\phi \gg 1$, $\Lambda \ll 1$,

$$\left.\begin{aligned} \bar{u}^2 &\simeq 1 - \Lambda \\ \bar{m} &\simeq \exp[-\phi\Lambda]. \end{aligned}\right\} \quad (14)$$

During the major deceleration where $\bar{m}$ approaches its limiting value ($\bar{m} \to \exp -\phi$, $\bar{u} \to 0$)

$$\frac{\phi}{n}\Lambda = 1. \quad (15)$$

These limiting solutions are apparent in Fig. 5 at the upper left where the lines of constant mass (shown for $n = 3$) have a slope of minus one. In this region it will be noted that the body can only penetrate a gas mass corresponding to $\Lambda = 1/(\phi/n)$.

Equations (12) and (13) are frequently applied to the meteor case for the estimation of luminous intensity variation [2].

$$I = \tau\left(-\frac{\mathrm{d}m}{\mathrm{d}t}\right)\frac{u^2}{2} \quad (16)$$

where τ is the so-called luminous efficiency.* Here we will consider only the conditions for a maximum intensity. Differentiating equation (16) with respect to Λ and equating to zero gives

$$\frac{5}{2}\frac{\mathrm{d}\ln\bar{u}^2}{\mathrm{d}\Lambda} + \frac{1}{\rho}\frac{\mathrm{d}\rho}{\mathrm{d}\Lambda} + \frac{\mathrm{d}\ln\bar{m}}{\mathrm{d}\Lambda} = 0.$$

For the case of meteor atmospheric entry

$$\frac{\mathrm{d}\rho}{\mathrm{d}\Lambda} = \frac{\rho}{\Lambda}$$

and the other terms may be evaluated from equation (12) and (13). The resulting condition for maximum absolute luminosity is [6]

$$\Lambda = \frac{\exp[-\phi/n\,(1-\bar{u}^2)]}{5/2 + (n-1)(\phi/n)\,\bar{u}^2} = \frac{(\bar{m})^{1/n}}{5/2 + (n-1)(\phi/n)\,\bar{u}^2}. \quad (17)$$

For low values of ϕ, this simplifies to

$$\Lambda = 0{\cdot}4 \text{ and } \bar{u} = 0{\cdot}818$$

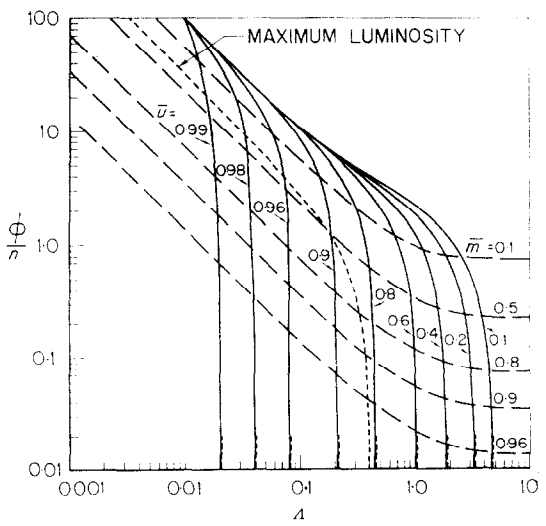

FIG. 5. Solution for constant $\overline{C_H}/\overline{C_D}$. Lines of constant mass ratio correspond to $n = 3$.

* The luminous efficiency can be assumed to be a function of velocity; this modifies slightly the conditions for maximum luminous intensity.

and for large values of ϕ

$$\phi\Lambda \simeq 1{\cdot}07 \quad \text{and} \quad \bar{m} \simeq 0{\cdot}34 \text{ (for } n = 3).$$

The condition for maximum luminous intensity is shown in Fig. 5 by the broken line.

Analytic solution for $\overline{C_H} = (\bar{D})^{-1/2}$

In the case of convective laminar ablation of a sphere moving at high velocity in a gas of uniform density (e.g. motion at constant altitude), the heat-transfer coefficient increases as the size of the sphere decreases:

$$\overline{C_H} = (\bar{D})^{-1/2}$$

or

$$\overline{C_H} = (\bar{m})^{-1/6}.$$

The drag coefficient is assumed to remain constant. Then equation (11) becomes

$$\frac{\mathrm{d} \ln \bar{m}}{\mathrm{d}\bar{u}^2} = \phi\,(\bar{m})^{-1/6}$$

which when integrated

$$\int_1^{\bar{m}} \frac{\mathrm{d}\bar{m}}{\bar{m}^{5/6}} = \phi \int_1^{\bar{u}^2} \mathrm{d}\bar{u}^2$$

yields

$$\bar{m} = \left[1 - \frac{\phi}{6}(1 - \bar{u}^2)\right]^6. \tag{18}$$

Just as in the solution presented in the previous section, the mass ratio is seen to depend only on the parameter ϕ and the velocity ratio. It will be noted that this relation results in a limiting mass ratio for $\phi < 6$

$$\lim_{\bar{u}\to 0} \bar{m} = \left(1 - \frac{\phi}{6}\right)^6.$$

For $\phi > 6$, the mass ratio becomes zero at a velocity ratio

$$\lim_{m\to 0} \bar{u} = \sqrt{\left(1 - \frac{6}{\phi}\right)}.$$

The velocity variation may be determined by substituting equation (18) in equation (8)

$$-\frac{\mathrm{d}\Lambda}{\mathrm{d} \ln \bar{u}^2} = \left[1 - \frac{\phi}{6}(1 - \bar{u}^2)\right]^2$$

and integrating

$$-\int_0^{\Lambda} \mathrm{d}\Lambda = \int_1^{\bar{u}^2} \frac{1}{\bar{u}^2}\left[1 - \frac{\phi}{6}(1 - \bar{u}^2)\right]^2 \mathrm{d}\bar{u}^2.$$

The result is

$$\Lambda = \left(1 - \frac{\phi}{6}\right)^2(-\ln \bar{u}^2) + \frac{\phi}{3}\left(1 - \frac{\phi}{6}\right)(1 - \bar{u}^2) + \frac{\phi^2}{72}(1 - \bar{u}^4). \tag{19}$$

The results of equations (18) and (19) are shown in Fig. 6 in the same format as the previous case in Fig. 5. Comparison of these two figures indicates that the increase of heat-transfer coefficient due to decreasing size has an appreciable effect only near the end of the motion where it results in slightly smaller values of the dimensionless depth Λ. Furthermore, while a finite mass always results in the previous case, here a zero mass can result for the larger values of ϕ (see above).

The conditions for maximum luminosity for this case (shown by the broken line in Fig. 6) are

$$\Lambda = \frac{\sqrt{\bar{m}}}{(5/2)\,\bar{m}^{1/6} + (1/2)\phi\,\bar{u}^2} \tag{20}$$

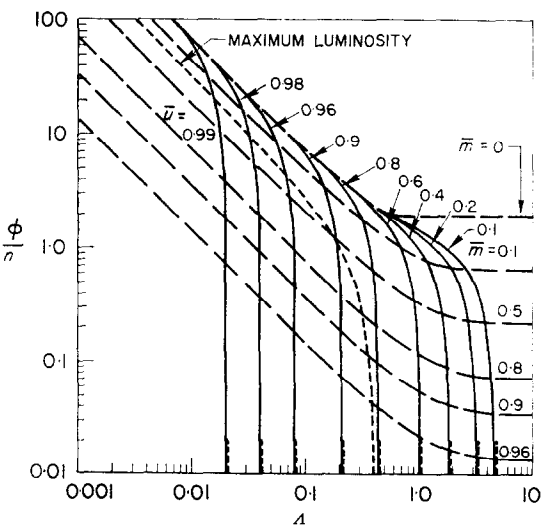

FIG. 6. Solution for $\overline{C_H}/\overline{C_D} = 1/\sqrt{D}$. Lines of constant mass ratio correspond to $n = 3$.

For small values of ϕ this simplifies to

$$\Lambda = 0{\cdot}4 \quad \text{and} \quad \bar{u} = 0{\cdot}818$$

just as in the previous case. For large values of ϕ

$$\phi\Lambda \simeq 1{\cdot}09 \quad \text{and} \quad \bar{m} \simeq 0{\cdot}3$$

which differs only slightly from the previous case.

Approximate analytic solution for $\overline{C_H} = k/\sqrt{(\bar{D})}\sqrt{(\Lambda)}$

For the two previous cases, an examination of Figs. 5 and 6 indicate that the major part of the mass loss occurs before the velocity has deviated appreciably from the simple solution for $\bar{m}/(\bar{C}_D\bar{A}) = 1$—i.e. a velocity variation given by

$$\bar{u} = \exp[-\Lambda/2] \tag{9}$$

This suggests the use of this velocity variation in approximate solutions for more complicated variations of the heat-transfer and drag coefficients. A case of interest is the convective laminar ablation of a sphere in atmospheric entry where

$$\overline{C_H} = \frac{k}{\sqrt{(\bar{D})}\sqrt{(\Lambda)}} = \frac{k}{(\bar{m})^{1/6}\sqrt{\Lambda}}$$

i.e. tends to increase with mass loss and to decrease with increasing gas density. The value of k in this expression corresponds approximately to $\sqrt{\Lambda}$ at the point where $\overline{C_H} = 1$. Thus k depends on, for example, the body size, the angle of atmospheric entry into the atmosphere, etc. With this variation of $\overline{C_H}$ and with the velocity variation given by equation (9), equation (4) becomes

$$-\frac{\mathrm{d}\bar{m}}{\mathrm{d}\Lambda} = \phi k \frac{\sqrt{(\bar{m})}\exp(-\Lambda)}{\sqrt{\Lambda}}$$

and integrating yields [7, 8]

$$\bar{m} = \left[1 - \frac{k\phi}{2}\int_0^{\Lambda} \frac{\exp(-\Lambda)}{\sqrt{\Lambda}}\,\mathrm{d}\Lambda\right]^2 \tag{12}$$

where the integral (shown in Fig. 7) may be

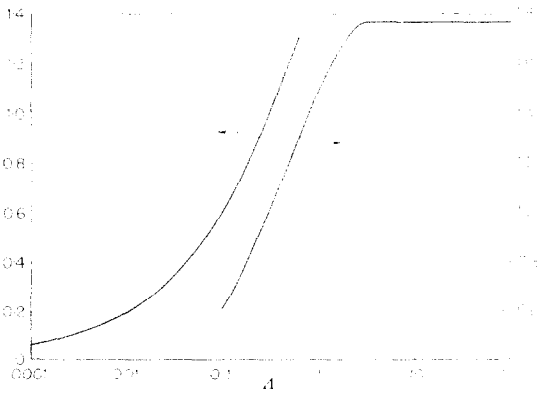

FIG. 7. Value of the integral $\int_0^{\Lambda} \frac{\exp -\Lambda}{\sqrt{\Lambda}}\,\mathrm{d}\Lambda$.

approximated for Λ small (say $\Lambda < 0{\cdot}02$) as

$$\int_0^{\Lambda} \frac{\exp(-\Lambda)}{\sqrt{\Lambda}}\,\mathrm{d}\Lambda \simeq 2\sqrt{\Lambda}$$

and for Λ large (say $\Lambda > 2$) as

$$\int_0^{\Lambda} \frac{\exp(-\Lambda)}{\sqrt{\Lambda}}\,\mathrm{d}\Lambda \simeq \sqrt{\pi}$$

The resulting mass variation, along with the assumed velocity variation is shown in the $\phi - \Lambda$ plane in Fig. 8. For this comparison, k was chosen as 0·005, corresponding to $\overline{C_H} = 1$ at an altitude of about 100 km. It is apparent that the effects of the decrease in the dimensionless heat-transfer coefficient due to increasing gas density dominate and result in appreciably lower rates of mass loss than in the previous cases discussed. Conditions for maximum luminosity for this case correspond to

$$5\Lambda + \frac{k\phi\exp(-\Lambda)\sqrt{\Lambda}}{\sqrt{m}} = 1 \tag{22}$$

and are shown by the broken line in Fig. 8. For small ϕ, equation (22) simplifies to

$$\Lambda = 0{\cdot}2 \quad \text{and} \quad \bar{u} = 0{\cdot}905$$

and for large ϕ to

$$\phi\sqrt{\Lambda} \simeq 97 \quad \text{and} \quad \bar{m} = 0{\cdot}27$$

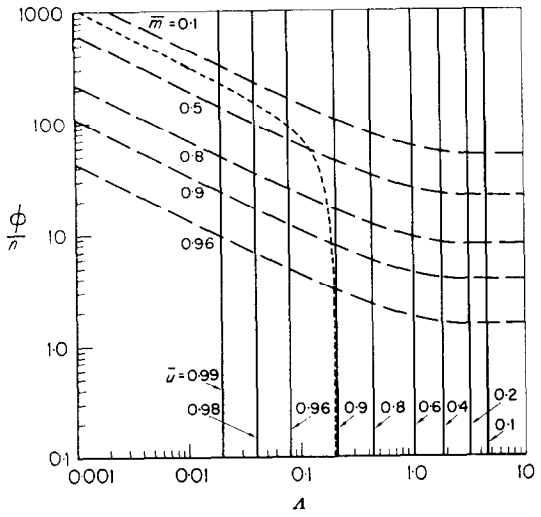

FIG. 8. Solution for $\overline{C_H}/\overline{C_D} = k/\sqrt{D}\sqrt{\Lambda}$ ($k = 0{\cdot}005$). Broken line shows conditions for maximum luminosity. Lines of constant mass ratio correspond to $n = 3$.

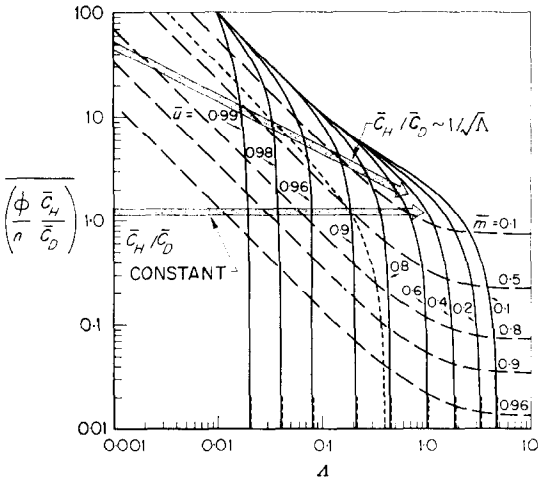

FIG. 9. Approximate general solution for variable $\overline{C_H}/\overline{C_D}$. Broken line shows conditions for maximum luminosity. Lines of constant mass ratio correspond to $n = 3$.

If the results of Fig. 8 are presented in terms of the average ablation efficiency from 0 to Λ,

$$\overline{\left(\frac{\phi}{n}\frac{\overline{C_H}}{\overline{C_D}}\right)} = \frac{1}{\Lambda}\int_0^{\Lambda}\left(\frac{\phi}{n}\frac{\overline{C_H}}{\overline{C_D}}\right)\mathrm{d}\Lambda$$

instead of the initial value (ϕ/n), they become almost identical to the results for constant $\overline{C_H}/\overline{C_D}$ shown in Fig. 5 for the region of major mass loss and major deceleration. This indicates that the analytic results for constant $\overline{C_H}/\overline{C_D}$ may also be used as an approximation for cases where the ratio varies appreciably. For the case of a body with variable $\overline{C_H}/\overline{C_D}$, the path of the body in the ϕ–Λ plane is no longer a horizontal line—but rather a line following the variation of the average value (from 0 to Λ) of $(\phi/n)(\overline{C_H}/\overline{C_D})$ with Λ. This is illustrated by the arrows in Fig. 9.

While this approximation will obviously fail in the final stages of the deceleration and mass-loss processes, it is useful for the tentative evaluation of cases where large variations of $\overline{C_H}/\overline{C_D}$ are expected. Machine computations are underway for various types of $\overline{C_H}$ and $\overline{C_D}$ variations in order to test the validity of the approximation.

III. APPLICATION TO LARGE METEORS

The meteor analysis for constant $\overline{C_H}/\overline{C_D}$ presented in the previous section has been applied by a number of authors to meteor data for the determination of atmospheric characteristics, high-velocity heat transfer, etc. [2, 3, 6]. In a previous paper [6], the author demonstrated that several unique features of the results shown in Fig. 6 could be exploited to determine meteor characteristics: (1) the initial variation of velocity with altitude is relatively independent of ϕ and can be used to determine the meteoroid's initial ballistic coefficient $(m/C_DA)_i$, and (2) the velocity ratio at which the maximum luminous intensity appears is indicative of the value of ϕ,

For larger meteoric bodies, where variation in the ratio $\overline{C_H}/\overline{C_D}$ is to be expected due to changes in flow regime and changes in the ablation mechanism, the approximate results indicated in Fig. 9 offer interesting possibilities. They indicate that the meteoroid's initial ballistic coefficient may be determined by the velocity variation with altitude and that the average value of the ablation efficiency, $(\phi/n)(\overline{C_H}/\overline{C_D})$, may be determined approximately from the velocity at maximum intensity.

Two recent well-observed meteors [9, 10] will be used as examples. Their velocity variation

with altitude, as determined photographically, is shown in Fig. 10. The arrows indicate the points of maximum luminosity.

The initial variation of velocity with altitude may be used to determine the initial entry velocity and the ballistic coefficient. The initial variation of velocity may be approximated by [see equation (14)]

$$\left(\frac{u}{u_i}\right)^2 \simeq 1 - \Lambda$$

Noting that, for atmospheric entry, the parameter Λ is

$$\Lambda = \frac{\rho}{\alpha} \frac{C_D A}{m \sin \theta}$$

it can be seen that plotting u^2 vs ρ yields u_i^2 as the intercept and $m/C_D A$ from the initial slope (using the scale height, α^{-1} from a standard atmosphere [11] and the measured value of the path angle, θ). This is shown for the two meteors in Fig. 11 and the resulting numerical values are indicated in Table 2. The determination of initial velocity and ballistic coefficient allows a representation in terms of the dimensionless parameters $\bar{u}$ and Λ, shown in Fig. 12. Comparison with the analytical results in Fig. 3 indicates good qualitative agreement with the theory.

The location of the points of maximum luminous intensity for these bodies on the ϕ–Λ

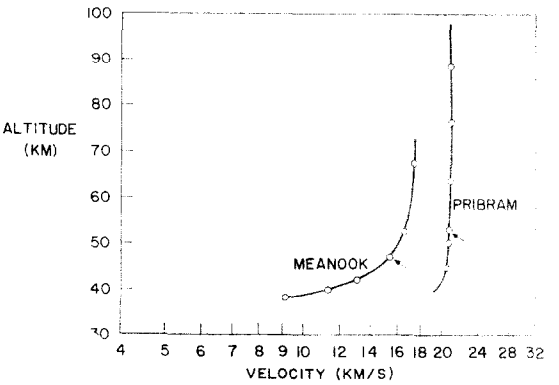

FIG. 10. Velocity variation with altitude for meteors.

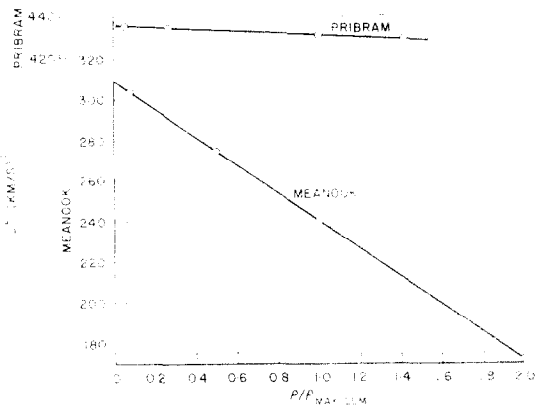

FIG. 11. Meteor data plotted to determine initial velocity and ballistic coefficient.

Table 2

Meteor	Time (s)	Velocity (km/s)	Altitude (km)	Angle θ (deg)	Comment	$\left(\frac{m}{C_D A}\right)_i$ (g/cm^2)
Pribram [9]	0	20·887	88·594	43°	Appeared at 97·8 km	76·2
	0·85806	20·864	76·289			
	0·85602	20·860	76·318			
	1·73230	20·838	65·837			
	2·49383	20·773	52·970			
	2·69203	20·717	50·164		Broke up at about 40 km	
	3·06758	20·459	44·858			
Meanook [10]	0	17·42	67·59	60·2		
	1·0	16·58	52·71		Flare at 0·8 s	5·61
	1·4	15·45	47·12			
	1·8	13·10	42·11		Broke in two at 1·75 s	
	2·0	11·28	39·98			
	2·2	9·16	38·21		Flare at 2·08 s	

map may be accomplished both from the values of $\bar{u}$ and A at that point. This is shown in Fig. 13. For both the Pribram [9] and Meanook [10] meteors, the corresponding values of $\bar{u}$ and A are in good agreement with the analytical results and allow determination of $(\phi/n)(\overline{C_H/C_D})$. There is seen to be a large difference in the resulting values of $(\phi/n)(\overline{C_H/C_D})$, a difference which is probably due to differences in body material.

The Pribram meteor [9] is a classic case—since it is the only large meteor observed photographically of which pieces were recovered after impact on the earth. The material was determined to be a chrondrite stone having a density of about 3·5 g/cm³. Using the determined ballistic coefficient, $(m/C_DA)_i = 76{\cdot}2$ g/cm² and assuming a spherical shape and a drag coefficient $C_D = 1$ yields an initial mass of 64100 g and a diameter of 32·7 cm. A total mass of about 7000 g was recovered and it was suspected [9] that one of the larger pieces was not found. It thus appears that more than 10 per cent of the original body survived atmospheric entry. Since the mass at maximum luminous intensity is about one third of the initial mass (see Fig. 13), it appears that the path of the body in the ϕ–A plane must have been downward with a slope close to minus one—as indicated by the arrow in Fig. 13. This trend can be rationalized by the expected reduction of the convective component of the heat-transfer coefficient with increasing gas density and of the radiative component with decreasing body size [8].

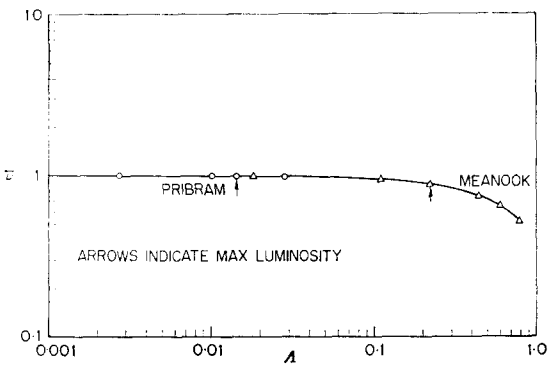

FIG. 12. Meteor data in terms of $\bar{u}$ and A.

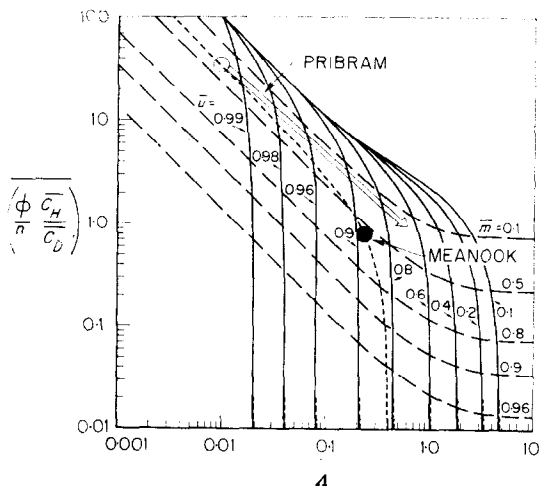

FIG. 13. Meteor results compared to the general solution.

REFERENCES

1. J. HOPPE, Die physikalischen Vorgänge bein Eindringen meteoritischer Körper in die Erdatmosphäre, *Astron. Nachr.* **262**, 169–198 (1937).
2. B. J. LEVIN, Elements of the physical theory of meteors, *Dokl. Akad. Nauk SSSR* **25**, 372–375 (1939). See also *Astron. Zh.* **17**, 12–41 (1940); **18**, 331–342 (1941).
3. V. A. BRONSHTEN, *Problems of the Motion of Large Meteoric Bodies in the Atmosphere*, Academy of Sciences of the USSR, Moscow (1963).
4. CARL GAZLEY JR., Heat-transfer aspects of the atmospheric re-entry of long-range ballistic missiles, *RAND* Report *R*-273, The RAND Corporation (1954).
5. H. J. ALLEN and A. J. EGGERS JR., A study of the motion and aerodynamic heating of missiles entering the atmosphere at high supersonic speeds, *NACA RM A23D28*, (1953).
6. CARL GAZLEY JR., Meteoric interaction with the atmosphere; theory of drag and heating and comparison with observations, Section 6 in *Aerodynamics of the Upper Atmosphere* compiled by D. J. MASSON, *RAND* Report *R*-339, The RAND Corporation (1959).
7. CARL GAZLEY JR., Atmospheric entry of manned vehicles, *RAND* Research Memorandum *RM*-2579, The RAND Corporation (1960). See also *Aerosp. Engng* **19**, 22–23, 90 (1960).
8. CARL GAZLEY JR., Atmospheric Entry, Chapter 10 of *Handbook of Astronautical Engineering* (ed. by H. H. KOELLE). McGraw-Hill, New York (1961).
9. ZD. CEPLECHA, Multiple fall of Pribram meteorites photographed, *Bull. Astron. Inst. Czech.* **12**, 21–47 (1961).
10. R. A. MILLMAN and A. F. COOK, Photometric analysis of a very slow meteor, *Astroph. J.* **130**, 648–662 (1959).
11. *U.S. Standard Atmosphere, 1962*. U.S. Government Printing Office (1962).

Résumé—Cet article examine les facteurs affectant la dynamique et la perte de masse de corps présentant une ablation pendant un mouvement à grande vitesse. La dynamique et l'ablation du corps sont interdépendantes, puisque la vitesse de perte de masse dépend de la vitesse et puisque la décélération dépend du rapport de la masse au produit de la surface du maître-couple par le coefficient de traînée (m/C_DA), qui peut changer à cause de la perte de masse et du changement de forme. L'énergie cinétique initiale du corps décroît à la fois à cause de la perte de masse et de la perte de vitesse. Les vitesses relatives de perte de masse et de perte de vitesse dépendent du "rendement" avec lequel l'énergie perdue due à la traînée aérodynamique est retournée au corps et absorbée dans le processus d'ablation.

Le cas classique du météore, où on suppose que l'écoulement est du type moléculaire libre avec des coefficients constants de transport de chaleur et de traînée, est passé en revue et présenté en fonction de paramètres sans dimensions qui permettent l'application à des cas autres que celui d'une entrée d'un météore dans l'atmosphère. Cette solution indique qu'une masse finie reste après la décélération, la grandeur de la masse relative à la masse initiale dépendant du "rendement" décrit ci-dessus.

En général, les cas avec des coefficients variables de transport de chaleur et de traînée demandent des solutions numériques à la machine (actuellement en cours). Cependant, des solutions analytiques pour certains cas sont possibles et sont présentées dans cet article. On obtient une solution analytique pour la variation spécifique du coefficient de transport de chaleur correspondant à une sphère avec un échauffement par convection laminaire en vol hypersonique à altitude constante. Dans ce cas, l'augmentation du coefficient sans dimensions de transport de chaleur due à la diminution de la taille du corps (augmentant ainsi effectivement le "rendement") peut aboutir à une perte complète de masse pendant le processus de décélération.

A la fois pour ce cas et le cas du météore, la variation de vitesse pendant la majorité de la perte de masse diffère seulement légèrement de celle pour un corps avec un coefficient balistique (m/C_DA) invariable. Cette approximation est utilisée pour formuler la solution analytique d'un cas qui correspond à l'échauffement par convection laminaire d'une sphère dans la rentrée hypersonique—c'est-à-dire un grand météore à faible vitesse ou une boule de feu. A cause de l'effet dominant de la décroissance du coefficient de transport de chaleur avec l'augmentation de la densité du fluide (diminuant ainsi effectivement le "rendement"), la vitesse de perte de masse est réduite et la masse finle est appréciable comparée à la masse initiale. Les résultats analytiques sont comparés avec deux boules de feu observées convenablement.

Zusammenfassung—Diese Abhandlung untersucht die Umstände, welche die Dynamik und den Massenverlust von Körpern beeinflussen, wenn sich diese mit sehr hoher Geschwindigkeit in der Atmosphäre bewegen und abschmelzen. Die Dynamik und das Abschmelzen des Körpers stehen untereinander in Beziehung, weil der Massenschwund von der Geschwindigkeit und die Verzögerung von dem Verhältnis Masse zu Widerstandsfläche (m/C_DA) abhängt, denn der den Widerstand verursachende Querschnitt kann sich sowohl durch Veränderung in der Form als auch durch den Massenverlust ändern. Die bezogenen Werte von Massenschwund und Geschwindigkeitsabnahme sind durch den "Wirkungsgrad" bedingt, mit welchem die durch den Strömungswiderstand verlorengegangene Energie wieder in den Körper zurückgeführt und durch den Abschmelzprozess absorbiert wird.

Der klassische Fall des Meteors, wo man eine Strömung freier Moleküle mit konstanter Wärmeübergangs- und Widerstandszahl annimmt, wird überprüft und in Termen mit gebräuchlichen dimensionslosen Parametern wiedergegeben. Damit ist die Anwendung auf Fälle, die anders geartet sind als das Auftreffen eines Meteors auf die Atmosphäre, möglich. In dieser Lösung treten eine endliche Masse auf, die nach dem Abbremsen übrigbleibt und der Betrag der Masse bezogen auf die Anfangsmasse, welche von dem oben bezeichneten "Wirkungsgrad" abhängt.

Im allgemeinen verlangen Fälle mit veränderlichen Wärmeübergangszahlen und Widerstandskoeffizienten numerische Lösungen durch Rechenmaschinen (jetzt im Fortschreiten begriffen). Es sind jedoch auch analytische Lösungen für bestimmte Fälle möglich und hier aufgeführt. Für die spezifische Änderung der Wärmeübergangszahl, die bei einer durch laminare Konvektion geheizten Kugel im Hyperschallflug in konstanter Höhe auftreten würde, ergibt sich eine analytische Lösung. In diesem Fall kann das Anwachsen der dimensionslosen Wärmeübergangszahl, verursacht durch die abnehmende Grösse des Versuchskörpers (der "Wirkungsgrad" wird erhöht) einen völligen Massenschwund beim Verzögerungsvorgang ergeben.

Für diesen Fall, wie auch für den des Meteors, unterscheidet sich die Änderung der Geschwindigkeit während des grössten Teils des Massenschwundes nur unbedeutend von der für einen Körper mit einem unveränderlichen ballistischen Koeffizienten (m/C_DA). Diese Näherung wird dazu verwendet,

eine analytische Lösung für einen Fall aufzustellen, der dem Wiedereintritt einer Kugel in die Atmosphäre entspricht, die dabei mit laminarer Konvektion beheizt wird und sich mit Hyperschallgeschwindigkeit fortbewegt, d.h. ein grosser, langsamer Meteor bzw. eine Sternschnuppe.

Wegen des vorherrschenden Einflusses der Abnahme der Wärmeübergangszahl bei steigender Dichte der Atmosphäre (der "Wirkungsgrad" wird verringert), wird die Massenverlustsrate herabgesetzt und die noch vorhandene Masse mit der Anfangsmasse in einer Abschätzung verglichen.

Die analytischen Ergebnisse werden mit zwei genau beobachteten Sternschnuppen verglichen.

Аннотация—В данной статье рассматриваются факторы, влияющие на динамику и потерю массы аблирующих тел при движении с большой скоростью. Динамика и абляция тела взаимозависимы, поскольку интенсивность потери массы зависит от скорости и поскольку торможение зависит от отношения массы к площади сопротивления (m/C_DA), которая может изменяться из-за потери массы и изменения формы. Относительная интенсивность потери массы и скорости зависит от «эффективности», с которой потеря энергии за счет гидродинамического сопротивления возвращается к телу и поглощается при абляции.

Классический случай метеора, где предполагают, что поток является свободномолекулярным при постоянных коэффициентах теплообмена и сопротивления, пересмотрен и представлен в виде общих безразмерных параметров, которые позволяют применять данный анализ для других случаев, а не только для случая вхождения метеора в атмосферу. Это решение дает конечную массу, оставшуюся после торможения, величину массы относительно начальной массе в зависимости от вышеуказанной «эффективности».

В общем, случаи переменных коэффициентов теплообмена и сопротивления требуют численных решений на электронно-счетной машине (в настоящее время эти вычисления производятся). Однако, аналитические решения некоторых случаев возможны и представлены в данной статье. Получено аналитическое решение для изменения коэффициента теплообмена, для шара при ламинарном конвективном нагреве при гиперзвуковых полетах с постоянной высотой. В этом случае увеличение безразмерного коэффициента теплообмена за счет уменьшения размера тела (таким образом, значительное увеличение «эффективности») может привести к полной потере массы при торможении.

Как в этом случае, так и в случае метеора, изменение скорости в течение основного периода потери массы только слегка отличается от этого периода для тела с неизменяющемся баллистическим коэффициентом (m/C_DA). Это приближение применялось для формулирования аналитического решения для случая, соответствующего ламинарному конвективному нагреву шара при возвращении в атмосферу с гиперзвуковой скоростью т.е. очень медленного метеора. За счет основного влияния уменьшения коэффициента теплообмена при увеличивающейся плотности потока (таким образом, значительно уменьшающейся «эффективности») скорость потери массы уменьшается, и конечная масса сравнима с начальной. Аналитические результаты сравнены с результатами, полученными для двух хорошо наблюдаемых метеоров.